Molecules and Cells

Oxymatrine Causes Hepatotoxicity by Promoting the Phosphorylation of JNK and Induction of Endoplasmic Reticulum Stress Mediated by ROS in L02 Cells

Li-li Gu[1,2], Zhe-lun Shen[1,2], Yang-Lei Li[1], Yi-Qi Bao[1], and Hong Lu[1,*]

[1]College of Pharmaceutical science, Zhejiang Chinese Medical University, Hangzhou 310053, Zhejiang Province, China, [2]These authors contributed equally to this work.
*Correspondence: luhong@zcmu.edu.cn
http://dx.doi.org/10.14348/molcells.2018.2180
www.molcells.org

Oxymatrine (OMT) often used in treatment for chronic hepatitis B virus infection in clinic. However, OMT-induced liver injury has been reported. In this study, we aim to investigate the possible mechanism of OMT-induced hepatotoxicity in human normal liver cells (L02). Exposed cells to OMT, the cell viability was decreased and apoptosis rate increased, the intracellular markers of oxidative stress were changed. Simultaneously, OMT altered apoptotic related proteins levels, including Bcl-2, Bax and pro-caspase-8/-9/-3. In addition, OMT enhanced the protein levels of endoplasmic reticulum (ER) stress makers (GRP78/Bip, CHOP, and cleaved-Caspase-4) and phosphorylation of c-Jun N-terminal kinase (p-JNK), as well as the mRNA levels of GRP78/Bip, CHOP, caspase-4, and ER stress sensors (IRE1, ATF6, and PERK). Pre-treatment with Z-VAD-fmk, JNK inhibitor SP600125 and N-acetyl-l-cysteine (NAC), a ROS scavenger, partly improved the survival rates and restored OMT-induced cellular damage, and reduced caspase-3 cleavage. SP600125 or NAC reduced OMT-induced p-JNK and NAC significantly lowered caspase-4. Furthermore, 4-PBA, the ER stress inhibitor, weakened inhibitory effect of OMT on cells, on the contrary, TM worsen. 4-PBA also reduced the levels of p-JNK and cleaved-caspase-3 proteins. Therefore, OMT-induced injury in L02 cells was related to ROS mediated p-JNK and ER stress induction. Antioxidant, by inhibition of p-JNK or ER stress, may be a feasible method to alleviate OMT-induced liver injury.

Keywords: apoptosis, ER stress, hepatotoxicity, JNK, L02 cell, oxymatrine

INTRODUCTION

Oxymatrine (OMT, $C_{15}H_{24}N_2O_2$) was a quinolizidine alkaloid extracted from traditional Chinese medicinal herbs such as Sophora flavescens and radix sophorae tonkinensis, which has been used in treating conditions like chronic viral hepatitis (Li et al., 1998), leukopenia caused by tumor radiation and chemotherapy (Ho et al., 2009) and plaque psoriasis (Zhou et al., 2017). As a chemically-defined natural product, some studies about OMT pharmacological effects have been developed, such as anti-prostate and colorectal cancer (Wang et al., 2017; Wu et al., 2015), anti-inflammatory (Sun et al., 2008), anti-cardiac, hepatic and renal fibrosis (Fu et al., 2016; Wang et al., 2016; Zhang et al., 2014), anti-virus (Jiang et al., 2017) and anti-arrhythmic effects (Cao et al., 2010). Apart from many findings of its beneficial activities, it was also reported that OMT worsened clinically relevant liver

Received 28 August, 2017; revised 23 December, 2017; accepted 16 January, 2018; published online 10 May, 2018

eISSN: 0219-1032

damage (Gao et al., 2002; Li and Huang, 2011; Tian, 2003). *In vitro*, 5mg/ml OMT have inhibitory action of hepatic cells (HL7702)' activity (Zhang et al., 2011), and animal experiments have shown that OMT (200 mg/kg) can trigger liver damage in ICR mice, the toxic mechanism is related to oxidative stress and apoptosis (Guo and Jin, 2016), so the underlining mechanisms remained to be further addressed.

In our previous work, we have found OMT at a dose of 160 and 320 mg/kg leads to obvious liver injury, which was related to the phosphorylation of c-Jun N-terminal kinase (p-JNK) signaling pathway mediated by tumor necrosis factor alpha (TNF-α) in mice liver. As we all known, JNK has a significant role in death receptor-initiated extrinsic as well as mitochondrial intrinsic apoptotic pathways (Dhanasekaran and Reddy, 2008). In human cells, multitudinous apoptotic stimuli, such as reactive oxygen species (ROS) and TNF-α, can trigger the activation of apoptosis signal-regulated kinase (ASK) 1, which eventually resulting to the JNK signalling cascade activation and apoptosis (Dai et al., 2017; Fukumoto et al., 2016). In additional, since the endoplasmic reticulum (ER) is an organelle for synthesis, folding and trafficking for protein, ER homeostasis is absolutely critical in hepatocytes, a major cell type rich in ER content (Han et al., 2016). Perturbation of these processes during different pathological states results in a condition known as ER stress, accompanying induced expression of several unfolded protein response (UPR) markers including Inositol-requiring enzyme 1 (IRE1), protein kinase RNA (PKR)-like endoplasmic reticulumkinase (PERK), activating of the transcription factor (ATF)6, glucose-regulated protein 78 (GRP78/Bip) and C/EBP homology protein (CHOP) (Ron and Walter, 2007). When sustained or unresolved ER stress appeared during the course of acute or chronic liver disease, it may account for hepatocyte dysfunction and death (Ozcan and Tabas, 2012).

Thus this study was designed to carry out the OMT-induced hepatotoxicity test in human normal liver cells (L02). And whether ROS-mediated JNK signaling pathway and ER stress induction or not was explored in L02 cells in response to treatment with OMT.

MATERIALS AND METHODS

Cell culture and reagents

L02 cells were purchased from the Cell Center of the Chinese Academy of Medical Sciences (China), and the cells were previously derived from the American Type Culture Collection (ATCC, USA). L02 cells were cultured and passed in RPMI 1640 medium (GIBCO, USA) supplemented with 10% fetal calf serum (FCS), 200 U/ml of penicillin sodium and 200 U/mL of streptomycin sulfate at 37℃ in a humidified atmosphere of 5% CO_2 in air.

OMT presents as a white powder, and its purity is 98%. OMT (lot number: ZY151018) was obtained from Shanghai Puzhen Biotechnology Co. Ltd, and diluted in the culture medium. Z-Val-Ala-Asp (OMe)-fluoromethylketone (Z-VAD-fmk, S7023), a pan-caspase inhibitor and SP600125 (S1460), a JNK inhibitor were obtained from Selleck (Shanghai, China), N-acetylcysteine (NAC, S0077, purity 98%), an antioxidant, was purchased from Beyotime Institute of Biotechnology (China), 4-phenylbutyric acid (4-PBA, Cl0041418, purity 98%), a ER Stress inhibiter was purchased from MACKLIN (China). Tunicamycin (TM, T818567, purity > 98%), a chemical inducer of UPR, was purchased from Solarbio (China).

MTT assay

Methyl thiazolyl tetrazolium (MTT) assay was used to detect the cell survival rate. Briefly, cells were seeded into a 96-well plate at a density of 2×10^4cells/ml, and divided into blank control, normal control and OMT group. Medium containing 6, 12, 18, 24 and 30 mmol/L of OMT was added into each well in a volume of 100 μL and at different time points (8, 16, 24 and 48 h), respectively. Four replicated wells were set up for each group. Then 20 μl MTT solutions (Sigma, Shanghai, China) was added into each well and followed by incubation at 37℃ for 4 h. The 150 μl of DMSO was further added to all of the wells after discarding culture medium. The optical density (OD) value was detected using a microplate reader (Bio-Rad, USA) at a wavelength of 570 nm. The experiments were performed in triplicate.

Hoechst 33342 staining assay

Hoechst 33342 staining was assayed morphological observation of nuclear change. Cells were seeded in 6-well plates at a density of 5×10^5 cell/ml, incubated with OMT for 24 h. The cell morphology was observed by Invert/phase contrast microscopy (MOTIC AE2000). Then the culture medium were removed and the cells were incubated with 0.5 mL Hoechst 33342 (Beyotime, China) (Yin et al., 2017) for 30 min at 37℃ in a humidified atmosphere of 5% CO_2 in air. After washed three times with PBS, the apoptotic cells were visualized using inverted fluorescence microscope (Nikon TE2000, Japan).

TdT-mediated dUTP Nick-End Labeling (TUNEL) assay

TUNEL assay (Dong et al., 2017) was performed on cells using the One Step TUNEL Apoptosis Assay Kit (Beyotime, China) according to the manufacturer's instructions. After OMT treatment, cells were fixed with 4% paraformaldehyde for 0.5 h and then stained with TUNEL reaction mixture for 1 h at 37℃ in the dark. The condensed or fragmented nuclei of apoptotic cells were observed using fluorescence microscopy at 200× magnification.

Annexin V/PI staining assay

The extent of apoptosis was measured through Annexin V-FITC apoptosis detection kit (Beyotime, China) as described in the manufacturer's instructions. After exposure to different concentrations of OMT for 24 h, cells were collected, washed twice with PBS, centrifuged for 5min, then gently resuspended in annexin V binding buffer (195 μl) and incubated with Annexin V-FITC (5 μl) and PI (10 μl) in dark for 15 min and analyzed by flow cytometry (BD, FACS Calibur, USA) using the Flo Max software.

ROS levels analysis

Fluorescent dye 2, 7-dichlorofluorescein-diacetate (DCFH-DA, Beyotime, China) was used to detect the intracellular ROS (Li et al., 2016). After exposed cells to OMT, Cells were washed

twice and loaded with DCFH-DA (10 μmol/L) and incubated at 37℃ for 20 min. The fluorescence of DCFH was measured on inverted fluorescence microscope at an excitation of 485 nm and emission of 520 nm.

Superoxide dismutase (SOD) activity and MDA content assay

The proteins from cells were collected after treated with OMT. The protein concentration was determined using the bicinchoninic acid protein assay kit (Beyotime, China). Cell homogenates were used for the determination of SOD and Lipid Peroxidation MDA levels by using a commercial kit (Beyotime, China). All procedures complied with the manufacturer's instructions. The results were corrected for their protein content.

Reverse transcription quantitative polymerase chain reaction (RT-qPCR)

Total RNA was extracted from cells using the RNAprep Pure Cell/Bacteria Kit (Tiangen, China). Reverse transcription of total RNA was carried out in a final volume of 20 μl, containing the following reagents (Tiangen, China): 5 × FastKing-RT SuperMix (4 μl) and RNase-free water. The reaction mixtures were then incubated at 42℃ (15 min) and 95℃ (3 min), and the cDNA samples were obtained. For PCR amplification, primers were designed. GAPDH sequences: 5'-ACAACTTT GGTATCGTGGAAGG-3' (forward primer) and 5'-GCCATCAC GCCACAGTTTC-3' (reverse primer); GRP78: 5'-CATCACGCC GTCCTATGTCG-3' (forward primer) and 5'-CGTCAAAGACC GTGTTCTCG-3' (reverse primer); CHOP: 5'-GGAAACAGAG TGGTCATTCCC-3' (forward primer) and 5'-CTGCTTGAGCCG TTCATTCTC-3' (reverse primer); Caspase-4: 5'-CAAGAGAAG CAACGTATGGCA-3' (forward primer) and 5'-AGGCAGATG GTCAAACTCTGTA-3' (reverse primer); PERK: 5'-ACGATGAGA CAGAGTTGCGAC-3' (forward primer) and 5'-ATCCAAGGC AGCAATTCTCCC-3' (reverse primer); IRE1:5'-CATCCCCATGC CGAAGTTCA-3' (forward primer) and 5'-CTGCTTCTCTCCGG TCAGGA-3' (reverse primer); ATF6:5'-TCCTCGGTCAGTGGA CTCTTA-3' (forward primer) and 5'-CTTGGGCTGAATTGAAG GTTTTG-3' (reverse primer). qPCR amplifications were carried out on a ABI 7500 Fast-time PCR system (Applied Biosystems, USA) using SuperReal PreMix Color (SYBR Green) (Tiangen, China) containing: 2× SuperReal Color PreMix, 50× ROX Reference Dye and RNase-Free ddH_2O, and using pre-optimized amplification conditions. Melting curve data were analyzed to determine PCR specificity. Relative fold expressions were analyzed using the $2^{-\Delta\Delta Ct}$ method and GAPDH Ct values as internal reference in each sample.

Western blot analysis

Cells were lysed using RIPA Lysis Buffer. Total protein samples were denatured and loaded on a SDS-polyacrylamide gel for electrophoresis, and transferred onto PVDF transfer membranes (Millipore, USA). Membranes were blocked and then incubated overnight at 4℃ with primary antibodies: Bax Rabbit mAb (#5023,CST), Bcl-2 Rabbit mAb (#4223, CST), pro-Caspase-9 Rabbit mAb (ab32068, abcam), Caspase-8 Rabbit mAb (#AF6442, Affinity), Caspase-3 (8G10) Rabbit mAb (#9665, CST), Phosphor-SAPK/JNK Rabbit mAb (#4668, CST), CHOP (L63F7) Mouse mAb (#2895, CST), Bip (C50B12) Rabbit mAb (#3177, CST), Caspase-4 Antibody (#4405, CST), β-action (C4) (sc-47778, Santa Cruz) at a 1:1,000 dilution in blocking solution. After three washings in TBST for each 10 min, the membranes were incubated with secondary horseradish peroxidase-conjugated goat anti-mouse/rabbit immunoglobulin G. Then the proteins were detected using an enhanced chemiluminescence detection kit. The images were obtained using Mini-PROTEAN gel imaging system (Bio-rad, USA).

Statistical analysis values

All data were presented as means ± SEM. Differences between the control and the treatment groups were determined using a one-way analysis of variance followed by the least significant difference test. The value of $P < 0.05$ and $P < 0.01$ were used as the criterion for statistical significance.

RESULTS

Effect of OMT on L02 cells viability

In order to evaluate OMT toxic effect on the L02 cells, the cell vitality was determined by MTT assay. As shown in Fig. 1, cells were treated with various concentrations of OMT at indicated times, the cell viability appeared in an obvious downtrend. Compared with control group, the OMT-treated group had significant statistical difference ($P < 0.05$, $P < 0.01$).The values of IC_{50} at 8, 16, 24 and 48 h were respectively 20.1 ± 4.5, 17.6 ± 1.7, 13.5 ± 1.9, 3.6 ± 0.7 mmol/L.

Effect of OMT on L02 cells morphology

The concentration of 6, 12, and 18 mmol/L were chose to observe the effect of OMT on cells morphology. As shown in

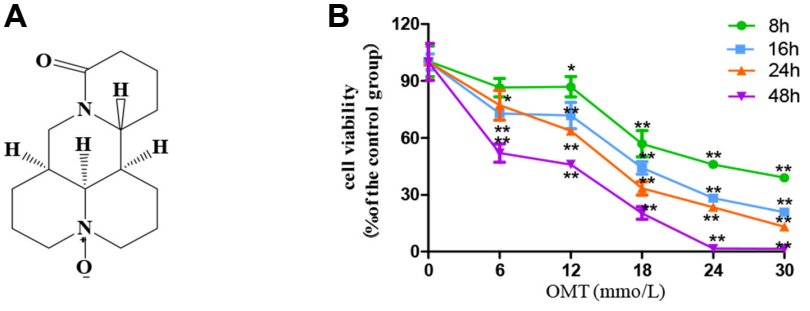

Fig. 1. Effect of OMT on cell viability in L02 cells. (A) Chemical structure of OMT; (B) Alterations seen in L02 cell survival rates after the cells were time-dependently treated with OMT (0, 6, 12, 18, 24 and 30 mmol/L). Data values were compared with control group. $*P < 0.05$, $**P < 0.01$.

Fig. 2A, no abnormality was observed in the cells from the control. Cells in OMT-treated groups, with increase of dose, change became more obviously, contour was gradually clear, cell diopter strengthened, the cytoplasm vacuolated, cells gradually became smaller and round, shrinking into the spherical, part of the cells was broken, and then fell off or suspended. Cell nucleus were stained with Hoechst 33342. In OMT (12 and 18 mmol/L) group (Fig. 2B), some nuclei were fracture or shrinkage, chromatin condensation and apoptotic body formation, prompting that OMT induced apoptosis, but apoptosis and necrosis were not completely independent, as they may share downstream pathways and signals.

Effect of OMT on L02 cells apoptosis

To further illuminate apoptosis, firstly apoptotic cells were detected by TUNEL analysis. Green fluorescence intensity that labeled apoptotic cells were exhibited markedly increased after OMT treatment for 24 h (Fig. 2C). The cell apoptosis rates were also detected by FCM analysis. The apoptosis rates had the tendency of increasing in a dose-dependent manner ($P < 0.05$), necrotic or post-apoptotic cells were in the majority (Figs. 2D and 2E), which was consistent with the result of TUNEL assay. Then the apoptotic proteins were detected by Western blotting. When cells were treated with different concentrations of OMT for 24 h, as shown in Figs. 3A and 3C, compared with 0 mmol/L OMT group, the expression of a pro-apoptotic protein Bax was up-regulated and an anti-apoptotic protein Bcl-2 was down-regulated in 18 mmol/L OMT-treated groups ($P < 0.05$), This change also appears apparently when cells were incubated with 10 mmol/L OMT at 24 and 48 h ($P < 0.05$, $P < 0.01$) (Figs. 3B and 3D). In addition, the levels of pro-Caspase-9 and -3 proteins in OMT-treated groups were decreased and cleaved ($P < 0.05$), but the levels of pro-Caspase-8 weren't obviously changed (Figs. 3E and 3G), which meant that activation of Caspase-8 was stagnated. As time prolonged, the levels of pro-Caspase-9, -3 and -8 proteins had a downward tendency with 10 mmol/L OMT treatment ($P < 0.05$, $P < 0.01$) (Figs. 3F and 3H).Caspase-8 is crucial for death receptor mediated apoptosis. Caspase-9 is necessary to trigger intrinsic apoptosis via the mitochondria pathway. Caspase-3 is required for efficient execution of apoptosis. Caspase-8 and -9 cleave Caspase-3 at the same site. These results hinted Caspase-9/3 induced intrinsic pathway may be mainly involved in OMT-induced injury in hepatocyte.

However, whether or not direct inhibition of Caspase activity protects against the injury was not tested. To address this potential issue, Z-VAD-fmk, a pan-caspase inhibitor, was used. After 24 h of incubation with OMT and Z-VAD-fmk,

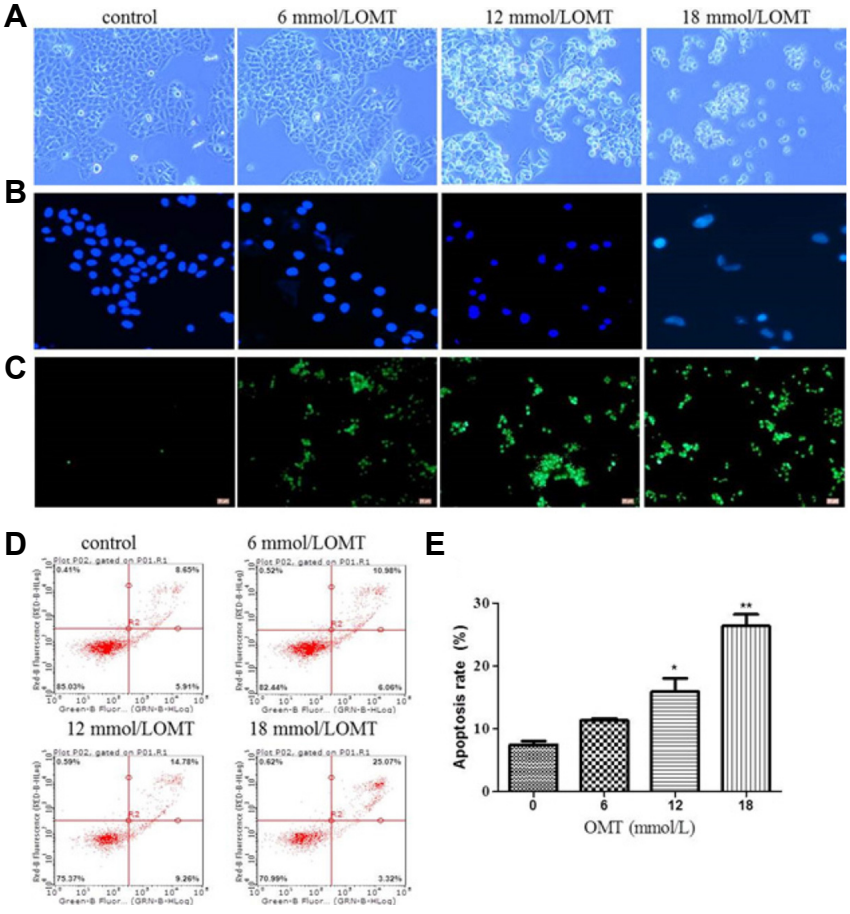

Fig. 2. Effect of OMT on cell morphology and apoptosis rate in L02 cells. L02 cells after treated with OMT (6, 12 and 18 mmol/L) for 24 h were observed by invert/phase contrast microscopy (scale bar: 100 μm) (A). Then cells stained with Hoechst 33342 (blue luminescence) (B) (scale bar: 200 μm) and TUNEL (green fluorescence) (C) (scale bar: 100 μm) were observed by fluorescence microscopy and stained with annexin V-FITC/PI and detected by flow cytometry (D). The apoptosis rate was calculated (E). $*P < 0.05$, $**P < 0.01$ vs the control group.

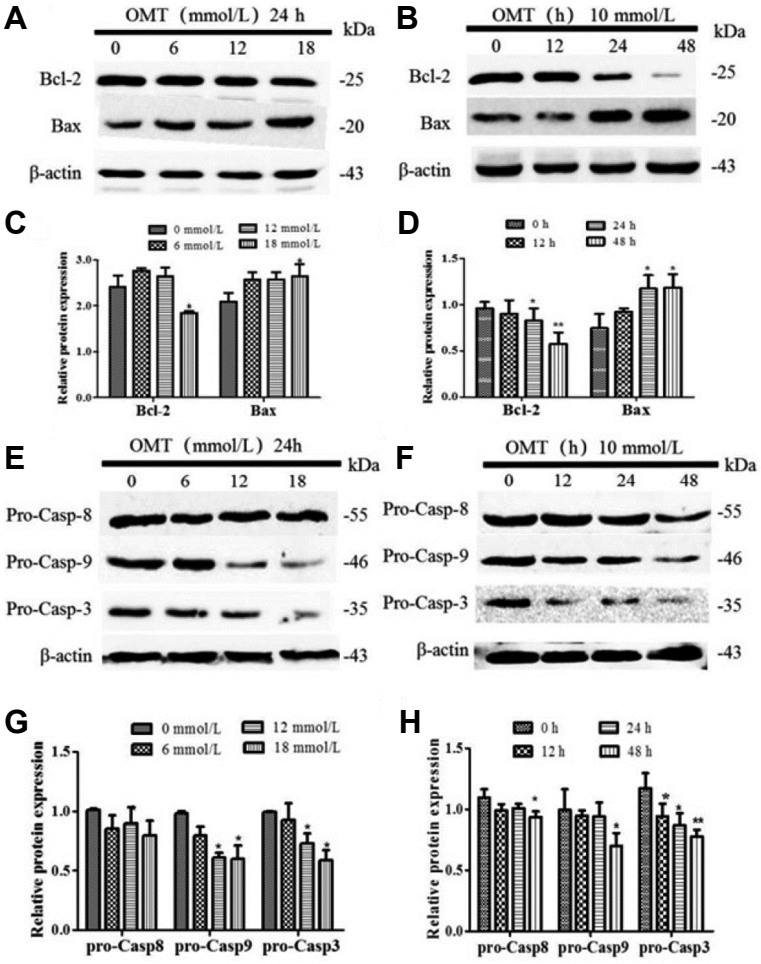

Fig. 3. Effect of OMT on apoptotic proteins in L02 cells. Cells were cultured with 0, 6, 12, 18 mmol/L of OMT for 24 h or 10 mmol/L OMT at 12, 24 and 48 h, and then all proteins were isolated from the cells. The expression of Bcl-2, Bax (A, B) and pro-caspase-9/-8/-3 (E, F) proteins were detected by western blotting and normalized to β-actin. Relative band intensities were used in order to quantify protein expression levels (C, D, G, and H). $*P < 0.05$, $**P < 0.01$ vs the control group.

compare with the OMT group, the cell ability was elevated, increased totally approximately by 15% (Fig. 4A), but it remained statistically significant compared with the control group ($P < 0.05$). Z-VAD-fmk inhibited OMT-induced cellular membrane blebbing (Fig. 4B). TUNEL analysis and Annexin V-FITC/PI staining showed the decreased in the number of apoptotic cells (Figs. 4C and 4D), but there are significant differences about the apoptosis rate between co-treatment with OMT and Z-VAD-fmk group and the normal control group ($P < 0.05$) (Fig. 4E). These results suggested that the pan-caspase inhibitor only partially blocked OMT-induced cell death. Moreover, cleavage of caspase-3 was cut down by the presence of caspases inhibitor ($P < 0.05$) (Fig. 4F). Consequently, the results clearly indicated that apoptotic induction of OMT in L02 cells was common mediated by caspases and non-caspases pathway.

Effect of OMT on oxidative stress markers in L02 cells

In order to determine whether OMT-induced apoptosis was related to oxidative stress in cells, we evaluated the intracellular ROS, MDA contents and SOD activity. Results are shown in Fig. 5, in comparison with the control group, the levels of ROS accumulated in OMT (12 and 18 mmol/L)-treated cells ($P < 0.05$, $P < 0.01$). In the OMT (18 mmol/L) -treated groups, the activity of SOD, as a frontline of antioxidant defense, were declined ($P < 0.01$), the levels of MDA, as a lipid peroxidation marker, were markedly elevated ($P < 0.05$).

Effect of OMT on JNK phosphorylation and ER stress associated protein expression in L02 cells

To investigate whether oxidative stress was accompanying with the activation of the JNK and ER stress pathways in cells in following OMT treatment, the expression of JNK phosphorylation and several markers of ER stress were detected by Western blotting. Compared with the control group, as shown in Fig. 6, when cells were treated with 0, 16, 12, 18 mmol/L of OMT for 24 h or 10 mmol/L OMT at 12, 24, 48 h, compared with the control group, OMT stimulated the phosphorylation of JNK expression ($P < 0.05$), particularly at 24 and 48 h treatment with 10 mmol/L OMT ($P < 0.01$) (Figs. 6A-6D). Simultaneously, the protein expression of ER molecular chaperone Bip/GRP78 had a rising trend, and the levels of CHOP protein, a key factor involved in ER stress-mediated apoptosis were notably elevated in 12, 18 mmol/L of OMT for 24 h ($P < 0.05$) and cleaved-caspase-4, a specific

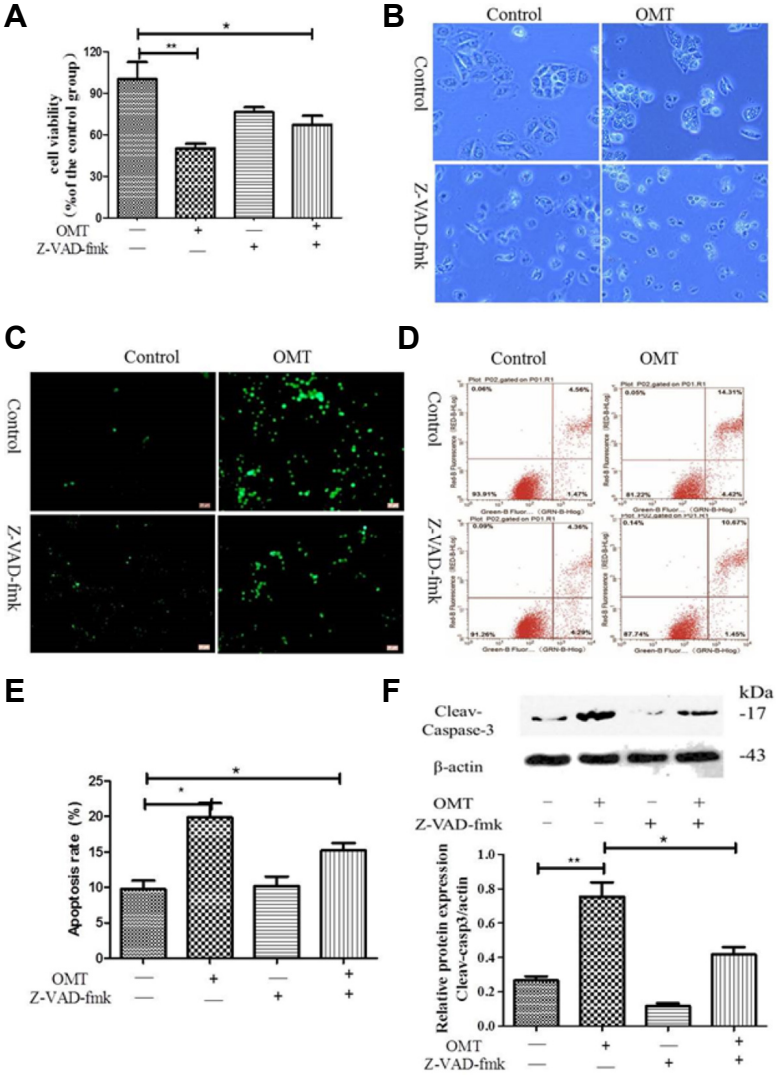

Fig. 4. Effect of caspase inhibitor z-VAD-fmk on the cell viability in OMT-treated cells. The cells in OMT (10 mmol/L) groups were pre-treatment with or without the pan-caspase inhibitor z-VAD-fmk (6 μmol/L). The cell ability was detected by MTT assay (A), The cell morphology was observed by Invert/phase contrast microscopy (scale bar: 100 μm) (B) and by Fluorescence Invert/phase contrast microscopy after staining with TUNEL (scale bar: 100 μm) (C), The cells stained with Annexin V-FITC/PI were detected by FCM (D), the apoptosis rate was calculated (E). Cleaved-caspase-3 protein was detected by western blotting and relative band intensities were used in order to quantify cleaved-caspase-3 protein expression levels (E). $**P < 0.01$, $*P < 0.05$ vs the control group.

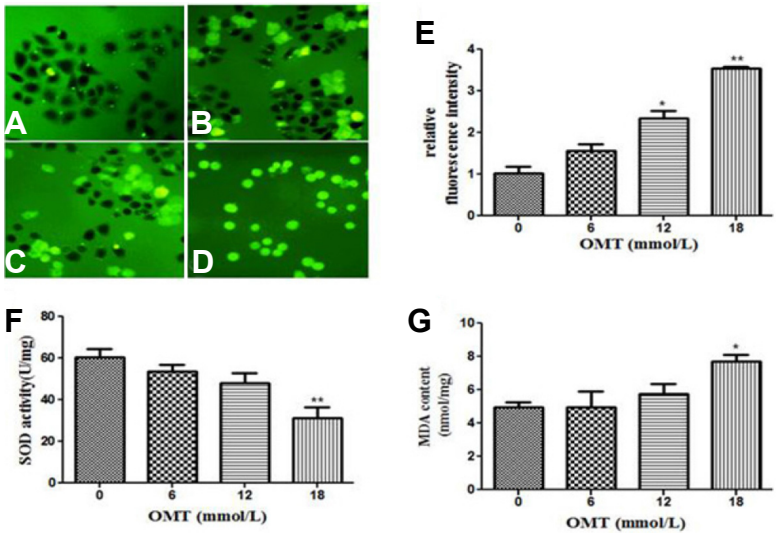

Fig. 5. Effect of OMT on oxidative stress in L02 cells. The cells were treated with 0, 6, 12 and 18 mmol/L of OMT (A-D) for 24 h and observed by Fluorescence microscope with fluorescent probe DCFH-DA (scale bar: 200 μm). The relative fluorescence intensity was quantified (E), SOD activity (F) and MDA content (G) were detected with reagent kits. $*P < 0.05$ and $**P < 0.01$, vs the control group.

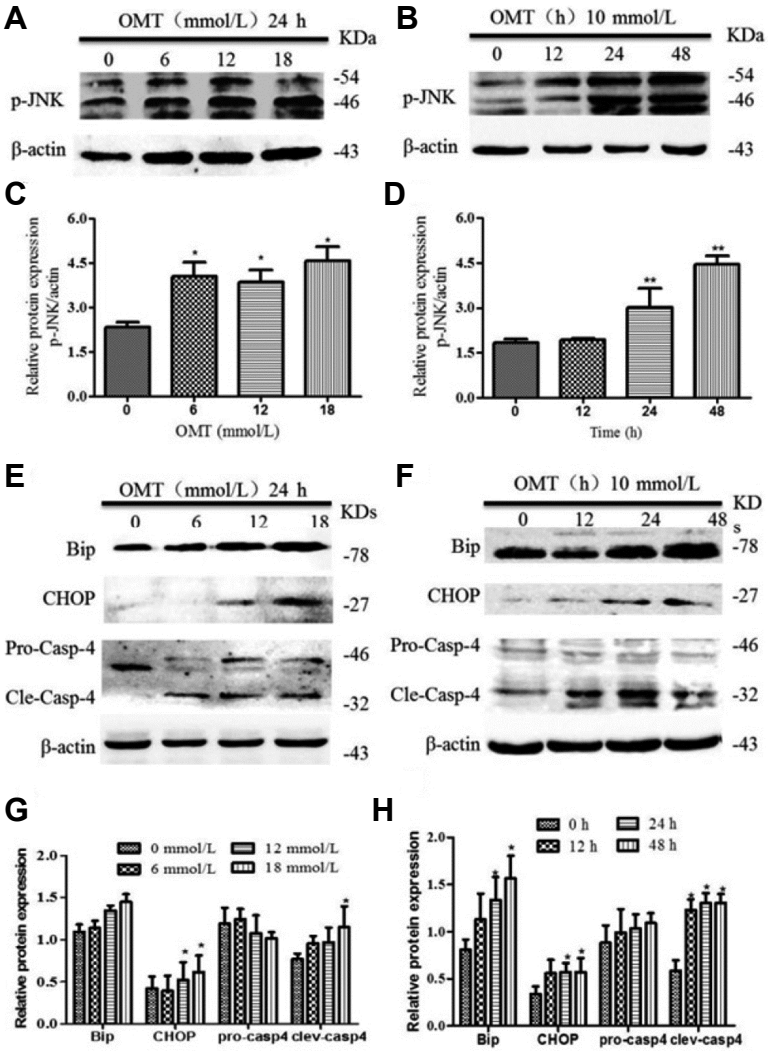

Fig. 6. Effect of OMT on JNK phosphorylation and other proteins involved in the ER stress response in L02 cells. Total cellular proteins were extracted from L02 cells culturedat 24 h after OMT (0, 6, 12, 18 mmo/L) treatment or at indicated times points after OMT (10 mmol/L) treatment respectively. The levels of p-JNK (A, B), Bip, CHOP and caspase-4 (E, F) was determined by western blot. β-actin was used as a loading control. Relative band intensities were used in order to quantify protein expression levels (C, D and G, H). *P < 0.05 vs the control group.

caspase protein in ER, were obviously increased ($P < 0.05$) (Figs. 6E and 6G). GRP78/Bip, CHOP and cleaved-caspase-4 showed an increasing trend with 10 mmol/L OMT treatment for 24 and 48 h ($P < 0.05$) (Figs. 6F and 6H). Together, these results indicated that the developmental exposure of cells to OMT induced toxic effect via the activation of CHOP, Caspase-4 and JNK signaling pathway.

Effect of OMT on the mRNA levels of ER stress makers in L02 cells

To further to the ER stress involved in OMT-induced cell death, we detected the mRNA levels of ER stress makers including GRP78/Bip, CHOP and Caspase 4 as well as three ER stress-signaling molecules PERK, IREI and ATF6.As shown in Fig. 7, With OMT concentration enrichment, OMT dramatically elevated the levels of GRP78/Bip, CHOP and IREI mRNA expression ($P < 0.05$, $P < 0.01$). The levels of Caspase-4 mRNA in 6 mmol/L OMT-treated group was higher than the other groups and increased significantly Compared with the normal group ($P < 0.01$) and dropped in 12 and 18 mmol/L OMT groups which were still higher than control. The levels of PERK mRNA in 12 and 18 mmol/L OMT groups raised and were notably different from the control ($P < 0.01$). The mRNA levels of ATF6 in 6 and 12 mmol/L OMT groups were also significantly elevated ($P < 0.01$, $P < 0.05$). IRE1, PERK and ATF6 are normally held in inactive states in ER membranes by binding to intra-ER chaperones, particularly the GRP78/Bip (Bertolotti et al., 2000). However, they promote the expression of genes required for folding of newly synthesized proteins and/or for degradation of unfolded proteins to reestablish homeostasis and normal ER function once ER stress occurs. The above ER stress related gene results were to some extent in accordance with the protein expression levels, and provided evidences to support this view that activation of ER stress pathways involves in OMT-induced cell damage.

Effect of SP600125 and NAC on OMT-induced cytotoxicity

To illuminate the relationship between the phosphorylation of JNK and OMT-induced cytotoxicity, we observed the cell

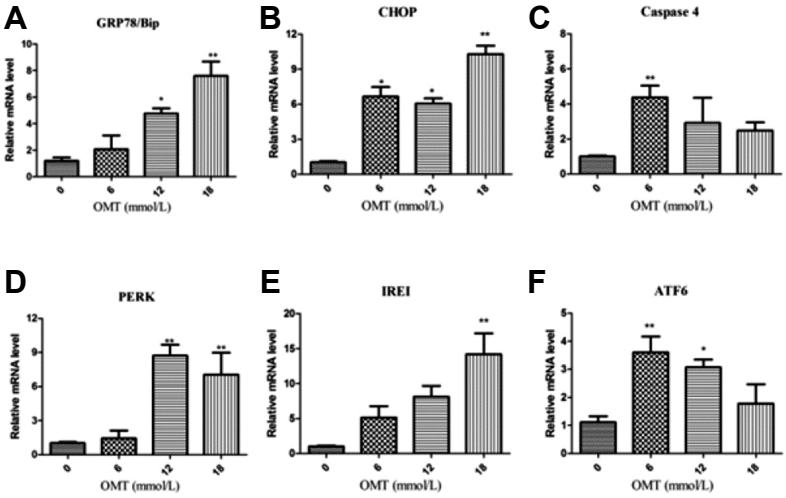

Fig. 7. Effect of OMT on the mRNA expression of ER stress-related genes in L02 cells. Total RNA was extracted at 24 h after OMT (0, 6, 12, 18 mmol/L) treatment. The mRNA levels of GRP78/Bip (A), CHOP (B), caspase-4 (C), PERK (D), IREI (E) and ATF6 (F) were determined by RT-qPCR. GAPDH was used as a loading control, Results are expressed as 2^{-ddCt} values. $*P < 0.05$, $**P < 0.01$ vs the control group.

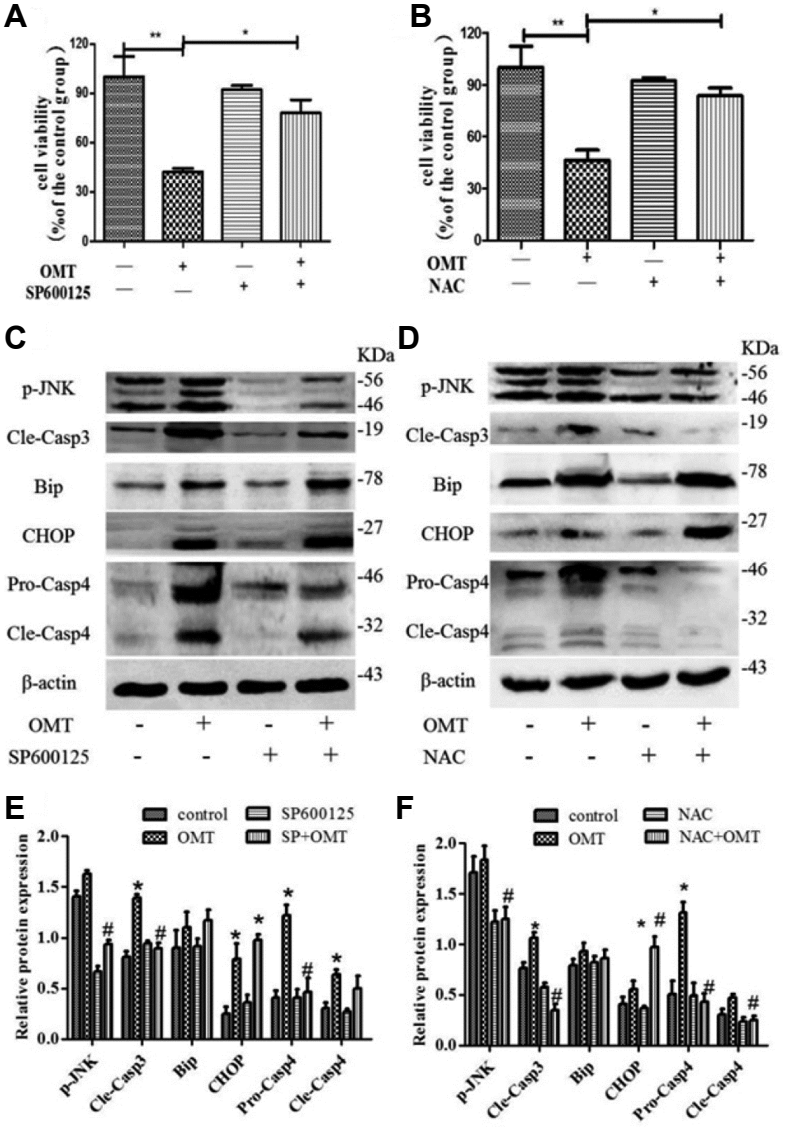

Fig. 8. Effect of SP600125 and NAC on cell viability and ER stress-related protein expression in OMT-treated L02 cells. Cells was pretreated with SP600125 (10 μmol/L) for 6 h or NAC (1 mmol/L) for 6 h, then treated with OMT (10 mmol/L) for 24 h. The cell viability was measured by MTT assay (A and B).ER stress related protein p-JNK, Bip, CHOP, caspase-4 and cleaved-caspase-3 expression were detected by western bloting (C and D). Relative band intensities were used in order to quantify protein expression levels (E and F). $*P < 0.05$, $**P < 0.01$ vs the control group, $^{\#}P < 0.05$ vs the OMT group.

viability and cleaved-capase-3 after pre-treatment with SP600125, a JNK inhibitor in OMT-treated cells. Compare with the OMT-treated group, SP600125 increased cell viability (Fig. 8A, $P < 0.05$), retarded the level of p-JNK protein and activation of Caspase-3 (Figs. 8C and 8E, $P < 0.05$).As we all known, JNK phosphorylation is to some extent induced in response to ER stress (Zhang et al., 2017). SP600125 decreased OMT-induced the expression levels of Caspase-4 protein ($P < 0.05$), had no obvious change the expressions of GRP78/Bip and CHOP (Figs. 8C and 8E), indicating that SP600125 has no intervention effect on the activation of Caspase-4 and CHOP induced by OMT.

In order to clarify whether accumulation of ROS will stimulate the phosphorylation of JNK and induce ER stress, leading to cell death. So we choose NAC, a ROS scavenger, compare with the OMT group, significantly increased cell viability (Fig. 8B, $P < 0.05$), decreaed the phosphorylation levels of JNK protein and activation of Caspase-3 ($P < 0.05$) (Figs. 8D and 8F). NAC further down-regulated markedly OMT-induced cleaved-caspase-4 protein expression ($P < 0.05$), and elevated the CHOP protein levels ($P < 0.05$),but did not change notably the levels of GRP78/Bip protein, which was still higher than the control group (Figs. 8D and 8F), suggesting that NAC relieved the OMT-induced injury through the inhibition of JNK phosphorylation and caspase-4 activation.

Effect of 4-PBA and TM on OMT-induced cytotoxicity

To investigate further, 4-PBA and TM were used to test with OMT exposed to cells respectively, and make sure the role of ER stress involved in OMT-induced cytotoxicity,. Results as shown in Fig. 9A, compare with the OMT group, co-treatment of 4-PBA (2 mmol/L) and OMT elevated the cell viability, increased totally approximately by 20% and alleviated cell morphology damage (Fig. 9B). Whereas, TM (1 μmol/L) had no effect on cell viability induced by OMT. When concentration of TM reached up to 2 μmol/L, compare with the control group, the cell viability was decreased ($P < 0.05$). The co-treatment of TM and OMT will be much worse for cell survival ($P < 0.01$), which indicated that ER stress inducer would aggravate OMT-induced cell damage and blocking ER stress could relieve it. In addition, as shown in Fig. 9C, co-treatment with 4-PBA decreased the levels of p-JNK and cleaved-caspase-3 proteins ($P < 0.05$), but had no effect of the expression of Bip protein in OMT-treated cells.

DISCUSSION

OMT, an alkaloid component extracted from the roots of Sophora species, has been shown various pharmacological effects such as anti-inflammatory, anti-fibrosis, and anti-tumor effects and the ability to protect against myocardial damage, etc (Lu et al., 2016b) and exhibits better prospect of clinical development. However the hepatotoxicity induced by OMT is attracting more attention. In order to guarantee its safe application, some in vitro cytotoxicity assays were conducted to explore its safety. L02 cells belong to human normal liver cells, and are anchorage-dependent and epithelioid cells, has became a important cell model to research all kinds of drug hepatotoxicity and damage mechanism. In this study, our findings first show that exposed cells to OMT decreased cell viability, manifested nuclear morphological change and increased apoptosis rate. ROS-caused oxidative stress is a common pathological physiological basis of liver disease with the joint action of cytokines (Ashraf and Sheikh, 2015). Then as we had expected, after treatment with OMT

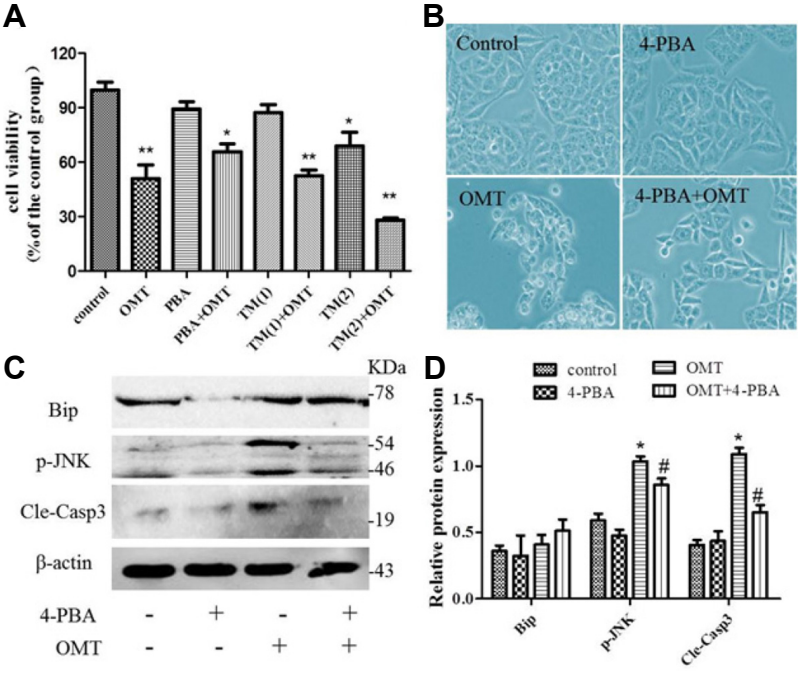

Fig. 9. Effect of 4-PBA in OMT-treated L02 cells. Cells was exposed to OMT (10 mmol/L) with 4-PBA (2 mmol/L) or TM (1 and 2 μmol/L) for 24 h, respectively. The cell viability was measured by MTT assay (A). $*P < 0.05$, $**P < 0.01$ vs the control group. Cell morphology after treatment with 4-PBA was observed by invert/phase contrast microscopy (scale bar: 200 μm) (B). The levels of p-JNK, GRP78/Bip and cleaved-caspase-3 protein in 4-PBA-treated group were detected by western blotting (C). Relative band intensities were used in order to quantify protein expression levels (D). $*P < 0.05$ vs the control group, $\#P < 0.05$ vs the OMT group.

of different concentrations, intracellular ROS levels and MDA contents appeared to go up and SOD activity declined, suggesting the toxic mechanism was related to oxidative stress and apoptosis.

The relative balance between the anti-apoptotic and pro-apoptotic family members influences the susceptibility of cells to a death signal. OMT-induced cytotoxicity accompyed with the up regulation of apoptotic protein Bax and down regulation of Bcl-2. As such, activation of caspase requires cleavage into smaller subunits under apoptotic conditions. The pro-caspase -3/-8/-9 levels reduced to convert into cleavage in response to OMT treatment, which were similar to that in HL-60 human leukemia cells (Liu et al., 2014). Z-VAD-fmk, a caspase inhibitor with near 100% efficacy in vivo, only partially weaken the cell death and lessen caspase-3 cleavege in OMT-treated group, indicating OMT-Induced injury was a common caspase and non-caspase dependent processing in vitro.

Several prior studies have described that ROS can mediate the sustained activation of JNK pathways (Chye et al., 2014; Schwabe and Brenner, 2006). JNK are important signaling molecules in multiple pathways in liver physiology and diseases (Seki et al., 2012). As we expected, exposed cells to OMT, a marked increase of p-JNK protein levels was observed, which was also consistent with the results *in vivo* (Lu et al., 2016a). Furthermore ER is also sensitive to oxidative stress. ER stress-induced cell toxicity plays an critical role in the development of drug-induced liver injury (Malhi and Kaufman, 2011; Wu et al., 2016). As we all known, faced with persistent ER stress, adaptation starts to fail and apoptosis occurs, possibly mediated through calcium perturbations, ROS (Kim et al., 2016), the pro-apoptotic transcription factor CHOP , the ER-resident caspase-4 and JNK phosphorylation (Borkham-Kamphorst et al., 2016). And there was not reported that ER stress signaling pathway involved in the clinical application of OMT (Lu et al., 2016c). In this experiment, we found that OMT can induce ER stress response as evidenced by up-regulation of the mRNA expression levels of ER stress sensors PERK, IREI and ATF6, and marker protein and mRNA expression levels of GRP78/Bip, CHOP and Caspase-4, which is an important issue to study and press forward.

The next step was to clarify whether or not direct inhibition of ROS-dependent JNK signalling pathway protects against the injury during the process. NAC is a source of glutathione and sulfhydryl groups, and a scavenger of free radicals due to its interaction with ROS. SP600125 is a broad spectrum JNK inhibitor for JNK1, JNK2 and JNK3 with IC50 of 40 nmol/L, 40 nmol/L and 90 nmol/L, respectively. In a cell based assay, the recommended concentration of SP600125 is 5-10 μmol/L (Wu et al., 2017). So NAC (1 mmol/L) and SP600125 (10 μmol/L) were applied respectively, the results demonstrated that NAC or SP600125 protect the liver cell from OMT through inhibition of JNK phosphorylation and caspase-3 activation. NAC may be useful in the management of non-paracetamol DILI, however, current available evidence is limited and does not allow for any firm (Chughlay et al., 2016). It is need for further research in this area.

Interestingly, activation of ER stress maker proteins (GRP78/Bip, CHOP) by OMT were not blocked by pretreatment with NAC or SP600125. Only cleavege of Caspase-4, an ER-resident caspase that has been previously associated with Caspase-3 activation in cases of ER-dependent apoptosis, was reduced by NAC, indicating that scavenging ROS resulted in inhibition of ER stress and partially restored cell viability and that OMT-induced ER stress may be independent of the phosphorylation of JNK. This inductive effect of OMT on liver cells was further proven by using 4-PBA and TM. It has been demonstrated that TM induced pharmacological ER stress and rapidly trans activated pleckstrin homology-like domain, family A, member-3 with a decrease in cell viability, which facilitates liver injury (Han et al., 2016). However, 4-PBA was administered to alleviate drug-induced injury in L02 cells via inhibition of the PERK-ATF4-CHOP pathway, thereby protecting against acute liver failure (Zhang et al., 2016a; 2016b). Our own data indicated that 4-PBA ameliorated OMT-induced cell death due to inhibition of JNK phosphorylation and Capase-3 activation, conversely, TM exacerbated OMT-induced cell growth inhibition.

In conclusion, the present study contributed to the existing knowledge that OMT-induced injury in L02 cells was related to ROS mediated JNK phosphorylation and the contribution of ER Stress. Antioxidant, suppression of JNK phosphorylation or ER stress inhibitor may be a potential detoxicant to liver damage induced by OMT and TCM containing OMT.

ACKNOWLEDGMENTS

The financial support for this study by the Medical Science and Technology project of Zhejiang Province (NO.2016ZB032) and National foundation preparatory research project of Zhejiang Chinese Medical University (NO.2016ZG12) is gratefully acknowledged.

REFERENCES

Ashraf, N.U., and Sheikh, T.A. (2015). Endoplasmic reticulum stress and Oxidative stress in the pathogenesis of Non-alcoholic fatty liver disease. Free Radic Res. *49*, 1405-1418.

Bertolotti, A., Zhang, Y., Hendershot, L.M., Harding, H.P., and Ron, D. (2000). Dynamic interaction of BiP and ER stress transducers in the unfolded-protein response. Nat. Cell Biol. *2*, 326-332.

Borkham-Kamphorst, E., Steffen, B.T., Van de Leur, E., Haas, U., Tihaa, L., Friedman, S.L., and Weiskirchen, R. (2016). CCN1/CYR61 overexpression in hepatic stellate cells induces ER stress-related apoptosis. Cell. Signal. *28*, 34-42.

Cao, Y.G., Jing, S., Li, L., Gao, J.Q., Shen, Z.Y., Liu, Y., Xing, Y., Wu, M.L., Wang, Y., Xu, C.Q., et al. (2010). Antiarrhythmic effects and ionic mechanisms of oxymatrine from Sophora flavescens. Phytother Res *24*, 1844-1849.

Chughlay, M.F., Kramer, N., Spearman, C.W., Werfalli, M., and Cohen, K. (2016). N-acetylcysteine for non-paracetamol drug-induced liver injury: a systematic review. Br. J. Clin. Pharmacol. *81*, 1021-1029.

Chye, S.M., Tiong, Y.L., Yip, W.K., Koh, R.Y., Len, Y.W., Seow, H.F., Ng, K.Y., Ranjit de, A., and Chen, S.C. (2014). Apoptosis induced by para-phenylenediamine involves formation of ROS and activation of p38 and JNK in chang liver cells. Environ Toxicol. *29*, 981-990.

Dai, X., Wang, L., Deivasigamni, A., Looi, C.Y., Karthikeyan, C., Trivedi,

P., Chinnathambi, A., Alharbi, S.A., Arfuso, F., Dharmarajan, A., et al. (2017). A novel benzimidazole derivative, MBIC inhibits tumor growth and promotes apoptosis via activation of ROS-dependent JNK signaling pathway in hepatocellular carcinoma. Oncotarget *8*, 12831-12842.

Dhanasekaran, D.N., and Reddy, E.P. (2008). JNK signaling in apoptosis. Oncogene *27*, 6245-6251.

Dong, R., Gong, Y., Meng, W., Yuan, M., Zhu, H., Ying, M., He, Q., Cao, J., and Yang, B. (2017). The involvement of M2 macrophage polarization inhibition in fenretinide-mediated chemopreventive effects on colon cancer. Cancer Lett. *388*, 43-53.

Fu, L., Xu, Y., Tu, L., Huang, H., Zhang, Y., Chen, Y., Tao, L., and Shen, X. (2016). Oxymatrine inhibits aldosterone-induced rat cardiac fibroblast proliferation and differentiation by attenuating smad-2,-3 and-4 expression: an in vitro study. BMC Complement. Altern. Med. *16*, 241.

Fukumoto, J., Jr.Cox, R., Fukumoto, I., Cho, Y., Parthasarathy, P.T., Galam, L., Lockey, R.F., and Kolliputi, N. (2016). Deletion of ASK1 protects against hyperoxia-induced acute lung injury. Plos One *11*, 1-13.

Gao, Z.W., Zhang, R.Q., and Liao, X.H. (2002). Two cases of aggravating liver damage caused by Oxymatrine injection in the patients with chronic hepatitis B. Adverse Drug Reactions J. 120-121.

Guo, Q.P., and Jin, R.M. (2016). Comparison of liver toxicity of matrine and oxymatrine in mice. Chin J. Pharmacol .Toxicol. *30*, 736-740.

Han, C.Y., Lim, S.W., Koo, J.H., Kim, W., and Kim, S.G. (2016). PHLDA3 overexpression in hepatocytes by endoplasmic reticulum stress via IRE1-Xbp1s pathway expedites liver injury. Gut *65*, 1377-1388.

Ho, J.W., Ngan Hon, P.L., and Chim, W.O. (2009). Effects of oxymatrine from Ku Shen on cancer cells. Anticancer Agents Med. Chem. *9*, 823-826.

Jiang, Y., Zhu, Y., Mu, Q., Luo, H., Zhi, Y., and Shen, X. (2017). Oxymatrine provides protection against Coxsackievirus B3-induced myocarditis in BALB/c mice. Antiviral Res. *141*, 133-139.

Kim, B., Kim, H.S., Jung, E.-J., Lee, J.Y., Tsang, B.K., Lim, J.M., and Song, Y.S. (2016). Curcumin induces ER stress-mediated apoptosis through selective generation of reactive oxygen species in cervical cancer cells. Mol. Carcinog. *55*, 918-928.

Li, J.L., and Huang, H.L. (2011). Epidemiological characteristics of adverse reaction of oxymatrine on database analyze. Anti-tumor Pharm. 149-152.

Li, J., Li, C., Zeng, M., Fan, J., Hua, J., Qiu, D., Xiao, S., She, X., and Li, G. (1998). Preliminary study on therapeutic effect of oxymatrine in treating patients with chronic hepatitis C. Chinese J. Integr. Med. *04*, 300.

Li, P., Zhang, L., Zhang, M., Zhou, C.Y., and Lin, N. (2016). Uric acid enhances PKC-dependent eNOS phosphorylation and mediates cellular ER stress: A mechanism for uric acid-induced endothelial dysfunction. Int. J. Mol. Med. *37*, 989-997.

Liu, J., Yao, Y., Ding, H., and Chen, R. (2014). Oxymatrine triggers apoptosis by regulating Bcl-2 family proteins and activating caspase-3/caspase-9 pathway in human leukemia HL-60 cells. Tumour Biol. *35*, 5409-5415.

Lu, H., Zhang, L., Gu, L.L., Hou, B.Y., and Du, G.H. (2016a). Oxymatrine induces liver injury through JNK signalling pathway mediated by TNF-alpha in vivo. Basic Clin. Pharmacol. Toxicol. *119*, 405-411.

Lu, M.L., Xiang, X.H., and Xia, S.H. (2016b). Potential signaling pathways involved in the clinical application of oxymatrine. Phytother. Res. 30, 1104-1112.

Lu, R.J., Zhang, Y., Tang, F.L., Zheng, Z.W., Fan, Z.D., Zhu, S.M., Qian, X.F., and Liu, N.N. (2016c). Clinical characteristics of drug-induced liver injury and related risk factors. Exp. Ther. Med. *12*, 2606-2616.

Malhi, H., and Kaufman, R.J. (2011). Endoplasmic reticulum stress in liver disease. J. Hepatol. *54*, 795-809.

Ozcan, L., and Tabas, I. (2012). Role of endoplasmic reticulum stress in metabolic disease and other disorders. Annu. Rev. Med. *63*, 317-328.

Ron, D., and Walter, P. (2007). Signal integration in the endoplasmic reticulum unfolded protein response. Nat. Rev. Mol. Cell Biol. *8*, 519-529.

Schwabe, R.F., and Brenner, D.A. (2006). Mechanisms of Liver Injury. I. TNF-alpha-induced liver injury: role of IKK, JNK, and ROS pathways. Am. J. Physiol. Gastrointest Liver Physiol. *290*, G583-589.

Seki, E., Brenner, D.A., and Karin, M. (2012). A liver full of JNK: signaling in regulation of cell function and disease pathogenesis, and clinical approaches. Gastroenterology *143*, 307-320.

Sun, H.L., Li, L., Shang, L., Zhao, D., Dong, D.L., Qiao, G.F., Liu, Y., Chu, W.F., and Yang, B.F. (2008). Cardioprotective effects and underlying mechanisms of oxymatrine against Ischemic myocardial injuries of rats. Phytother. Res. *22*, 985-989.

Tian, J.H. (2003). Worsened hepatitis B due to sophocarpidine capsula. Adverse Drug Reactions J. 407-408.

Wang, H.W., Shi, L., Xu, Y.P., Qin, X.Y., and Wang, Q.Z. (2016). Oxymatrine inhibits renal fibrosis of obstructive nephropathy by downregulating the TGF-beta1-Smad3 pathway. Ren Fail *38*, 945-951.

Wang, X., Liu, C., Wang, J., Fan, Y., Wang, Z., and Wang, Y. (2017). Oxymatrine inhibits the migration of human colorectal carcinoma RKO cells via inhibition of PAI-1 and the TGF-beta1/Smad signaling pathway. Oncol. Rep. *37*, 747-753.

Wu, C., Huang, W., Guo, Y., Xia, P., Sun, X., Pan, X., and Hu, W. (2015). Oxymatrine inhibits the proliferation of prostate cancer cells in vitro and in vivo. Mol. Med. Rep. *11*, 4129-4134.

Wu, F.L., Liu, W.Y., Van Poucke, S., Braddock, M., Jin, W.M., Xiao, J., Li, X.K., and Zheng, M.H. (2016). Targeting endoplasmic reticulum stress in liver disease. Expert Rev. Gastroenterol. Hepatol. *10*, 1041-1052.

Wu, Y., Li, Y., Shang, M., Jian, Y., Wang, C., Bardeesi, A.S., Li, Z., Chen, T., Zhao, L., Zhou, L., et al. (2017). Secreted phospholipase A2 of Clonorchis sinensis activates hepatic stellate cells through a pathway involving JNK signalling. Parasit. Vectors *10*, 147.

Yin, Z., Ding, H., He, E., Chen, J., and Li, M. (2017). Up-regulation of microRNA-491-5p suppresses cell proliferation and promotes apoptosis by targeting FOXP4 in human osteosarcoma. Cell Prolif. *50*.

Zhang, Q., Li, F.J., Jin, R.M., and Song, Z.P. (2011). Study on the Hepatotoxicity Induced by Matrine and Oxymatrine. Chinese Archives of Traditional Chinese Med. *29*, 1222-1225.

Zhang, S., Wu, J., Wang, H., Wang, T., Jin, L., Shu, D., Shan, W., and Xiong, S. (2014). Liposomal oxymatrine in hepatic fibrosis treatment: formulation, *in vitro* and *in vivo* assessment. AAPS PharmSciTech *15*, 620-629.

Zhang, L., Ren, F., Zhang, X.Y., Wang, X.X., Shi, H.B., Zhou, L., Zheng, S.J., Chen, Y., Chen, D.X., Li, L.Y., et al. (2016a). Peroxisome proliferator-activated receptor alpha acts as a mediator of endoplasmic reticulum stress-induced hepatocyte apoptosis in acute liver failure. Dis. Model. Mech. *9*, 799-809.

Zhang, W.P., Chen, L.H., Shen, Y.X., and Xu, J.M. (2016b). Rifampicin-induced injury in L02 cells is alleviated by 4-PBA via

inhibition of the PERK-ATF4-CHOP pathway. Toxicol. in vitro *36*, 186-196.

Zhang, B., Gao, C., Li, Y., and Wang, M. (2017). D-chiro-inositol enriched Fagopyrum tataricum (L.) Gaench extract alleviates mitochondrial malfunction and inhibits ER stress/JNK associated inflammation in the endothelium. J. Ethnopharmacol. *214*, 83-89.

Zhou, H., Shi, H.J., Yang, J., Chen, W.G., Xia, L., Song, H.B., Bo, K.P., and Ma, W. (2017). Efficacy and relapse-suppression of severe plaque psoriasis by oxymatrine: Results from a single blinded randomized controlled clinical trial. Br. J. Dermatol. *176*, 1446-1455.